

<sup>1</sup> **The Morphological Diversification of Siphonophore Tentilla**

<sup>3</sup> Alejandro Damian-Serrano<sup>1,‡</sup>, Steven H.D. Haddock<sup>2</sup>, Casey W. Dunn<sup>1</sup>

<sup>4</sup> <sup>1</sup> Yale University, Department of Ecology and Evolutionary Biology, 165 Prospect St.,  
<sup>5</sup> New Haven, CT 06520, USA

<sup>6</sup> <sup>2</sup> Monterey Bay Aquarium Research Institute, 7700 Sandholdt Rd., Moss Landing, CA  
<sup>7</sup> 95039, USA

<sup>8</sup> <sup>‡</sup> Corresponding author: Alejandro Damian-Serrano, email: alejandro.damianserrano@  
<sup>9</sup> yale.edu

<sup>10</sup> **Keywords**

<sup>11</sup> Siphonophora, tentilla, nematocysts, character evolution

<sub>12</sub> **Abstract**

<sub>13</sub> Siphonophores are free-living predatory colonial hydrozoan cnidarians found in every ocean  
<sub>14</sub> of the world. Siphonophore tentilla (tentacle side branches) are unique biological structures  
<sub>15</sub> for prey capture, composed of a complex arrangement of cnidocytes (stinging cells) bearing  
<sub>16</sub> different types of nematocysts (stinging capsules) and auxiliary structures. Tentilla present  
<sub>17</sub> an extensive morphological and functional diversity across species. While associations  
<sub>18</sub> between tentilla form and diet have been reported, the evolutionary history giving rise to this  
<sub>19</sub> morphological diversity is largely unexplored. Here we examine the evolutionary gains and  
<sub>20</sub> losses of novel tentillum substructures and nematocyst types on the most recent siphonophore  
<sub>21</sub> phylogeny. Tentilla have a precisely coordinated high-speed strike mechanism of synchronous  
<sub>22</sub> unwinding and nematocysts discharge. Here we characterize the kinematic diversity of this  
<sub>23</sub> prey capture reaction using high-speed video and find relationships with morphological  
<sub>24</sub> characters. Since tentillum discharge occurs in synchrony across a broad morphological  
<sub>25</sub> diversity, we evaluate how phenotypic integration is maintaining character correlations across  
<sub>26</sub> evolutionary time. We found that the tentillum morphospace has low dimensionality, we  
<sub>27</sub> identified instances of heterochrony and morphological convergence, and generated hypotheses  
<sub>28</sub> on the diets of understudied siphonophore species. Our findings indicate that siphonophore  
<sub>29</sub> tentilla are phenotypically integrated structures with a complex evolutionary history leading to  
<sub>30</sub> a phylogenetically-structured diversity of forms which are predictive of kinematic performance  
<sub>31</sub> and feeding habits.

<sup>32</sup> **Introduction**

<sup>33</sup> Siphonophores have fascinated zoologists for centuries for their extremely subspecialized  
<sup>34</sup> colonial organization and integration. Today we have a comprehensive taxonomic coverage  
<sup>35</sup> on the morphological diversity of this group due to the extensive work of siphonophore  
<sup>36</sup> taxonomists in the past few decades (Pugh, 1983, 2001; Pugh & Harbison, 1986; Pugh  
<sup>37</sup> & Youngbluth, 1988; Hissmann, 2005; Haddock *et al.*, 2005; Dunn *et al.*, 2005; Bardi &  
<sup>38</sup> Marques, 2007; Pugh & Haddock, 2010; Pugh & Baxter, 2014), which has been elegantly  
<sup>39</sup> synthesized in detailed synopses (Totton & Bargmann, 1965; Mapstone, 2014). In addition,  
<sup>40</sup> recent advances in phylogenetic analyses of siphonophores (Munro *et al.*, 2018; Damian-  
<sup>41</sup> Serrano *et al.*, 2020) have provided a macroevolutionary context to interpret this diversity.  
<sup>42</sup> With these assets in hand, we can now begin to study siphonophores from an orthogonal  
<sup>43</sup> perspective, focusing on the diversity and evolutionary history of specific structures. Here we  
<sup>44</sup> focus on one of such structures: the tentilla. Like many cnidarians, siphonophore tentacles  
<sup>45</sup> bear side branches (tentilla) with nematocysts (Fig. 1C-E). But unlike other cnidarians,  
<sup>46</sup> most siphonophore tentilla are dynamic structures that react to prey encounters by rapidly  
<sup>47</sup> unfolding the nematocyst battery to slap around the prey (Fig. 1F). This maximizes the  
<sup>48</sup> surface area of contact between the nematocysts and the prey they fire upon. In addition,  
<sup>49</sup> siphonophore tentilla present a remarkable diversity of morphologies (Fig. 2), sizes, and  
<sup>50</sup> nematocyst complements (Fig. 3). Our overarching aim is to organize all this phenotypic  
<sup>51</sup> diversity in a phylogenetic context, and identify the evolutionary processes that generated it.

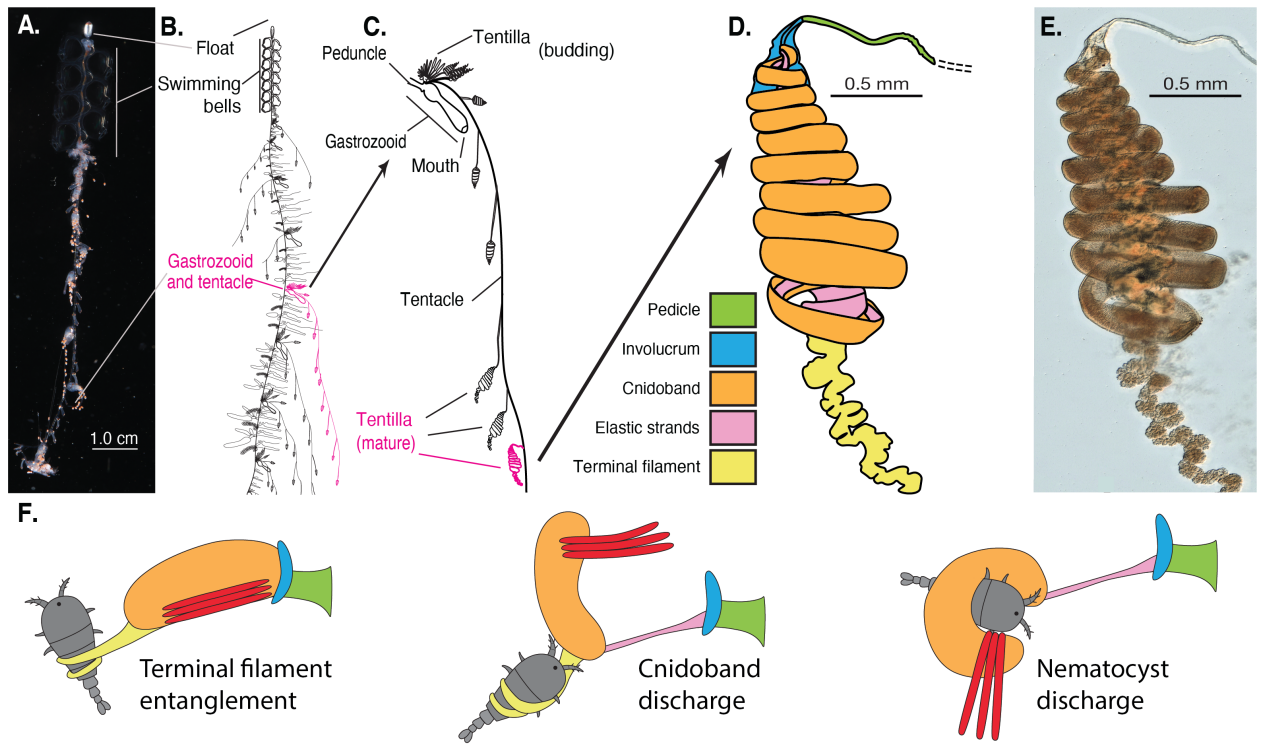


Figure 1: Siphonophore anatomy. A - *Nanomia* sp. siphonophore colony (photo by Catriona Munro). B, C - Illustration of a *Nanomia* colony, gastrozooid, and tentacle closeup (by Freya Goetz). D - *Nanomia* sp. Tentillum illustration and main parts. E - Differential interference contrast micrograph of the tentillum illustrated in D. Figure reproduced from Damian-Serrano et al. 2020 with permission. F. Action strip showing the behavior of tentilla during prey capture, illustrated by Riley Thompson.

52 In Damian-Serrano *et al.* (2020), we collected the most extensive morphological dataset  
53 on siphonophore tentilla and nematocysts using state-of-the-art microscopy techniques, and  
54 expanded the taxon sampling of the phylogeny to disentangle the evolutionary history. The  
55 analyses we carried out led to novel, generalizable insights into the evolution of pred-  
56 atory specialization. The primary findings of that work were that generalists evolved from  
57 crustacean-specialist ancestors, and that feeding specializations were associated with distinct  
58 modes of evolution and character integration patterns. The work we present here is comple-  
59 mentary to Damian-Serrano *et al.* (2020), showcasing a far more detailed account on the  
60 evolutionary history of tentilla morphology.

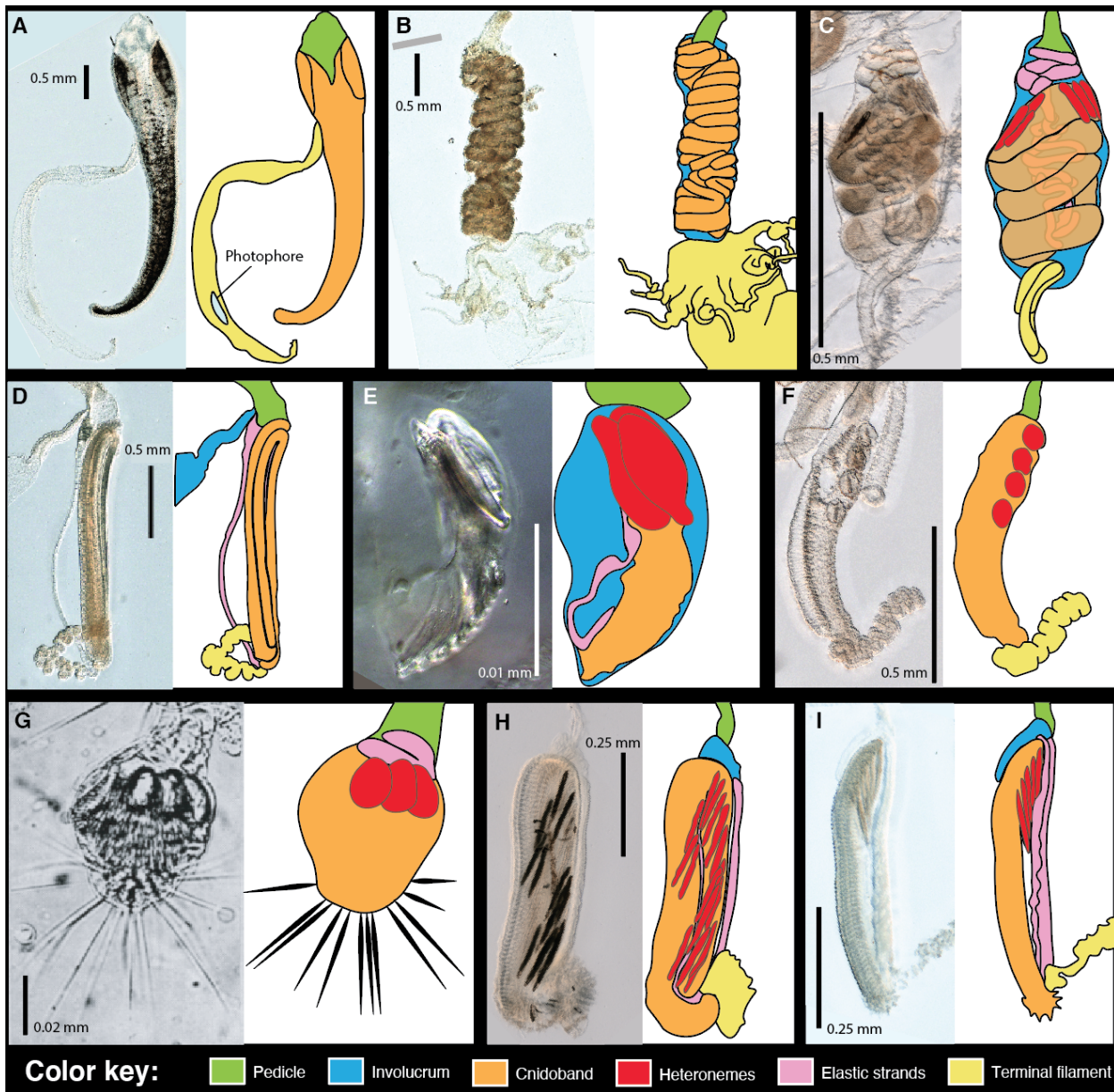


Figure 2: Tentillum diversity. The illustrations delineate the pedicle, involucrum, cnidoband, elastic strands, terminal structures. Heteroneme nematocysts (stenoteles in C,E,F,G and mastigophores in H,I) are only depicted for some species. A - *Erenna laciiniata*, 10x. B - *Lychnagalma utricularia*, 10x. C - *Agalma elegans*, 10x. D - *Resomia ornicephala*, 10x. E - *Frillagalma vityazi*, 20x. F - *Bargmannia amoena*, 10x. G - *Cordagalma* sp., reproduced from Carré 1968. H - *Lilyopsis fluoracantha*, 20x. I - *Abylopsis tetragona*, 20x.

61 Nematocysts are unique biological weapons for defense and prey capture exclusive to  
62 the phylum Cnidaria. Mariscal (1974) reported that hydrozoans have the largest diversity  
63 of nematocyst types among cnidarians. Among them, siphonophores present the greatest  
64 variety of types (Mapstone, 2014), and vary widely across taxa in which and how many types  
65 they carry on their tentacles (Fig. 3). Werner (1965) noted that there are nine types of  
66 nematocyst found in siphonophores, of which four, anacrophore rhopalonemes, acrophore  
67 rhopalonemes, homotrichous anisorrhizas, and birhopaloids, are unique to them. Heteroneme  
68 and haploneme nematocysts serve penetrant and entangling functions, while rhopalonemes  
69 and desmonemes work by adhering to the surface of the prey. While recent descriptive  
70 studies have expanded and confirmed our understanding of this diversity, the evolutionary  
71 history of nematocyst type gain and loss in siphonophores remains unexplored. Thus, here  
72 we reconstruct the evolution of shifts, gains, and losses of nematocyst types, subtypes, and  
73 other major categorical traits that led to the extant diversity we see in siphonophore tentilla.

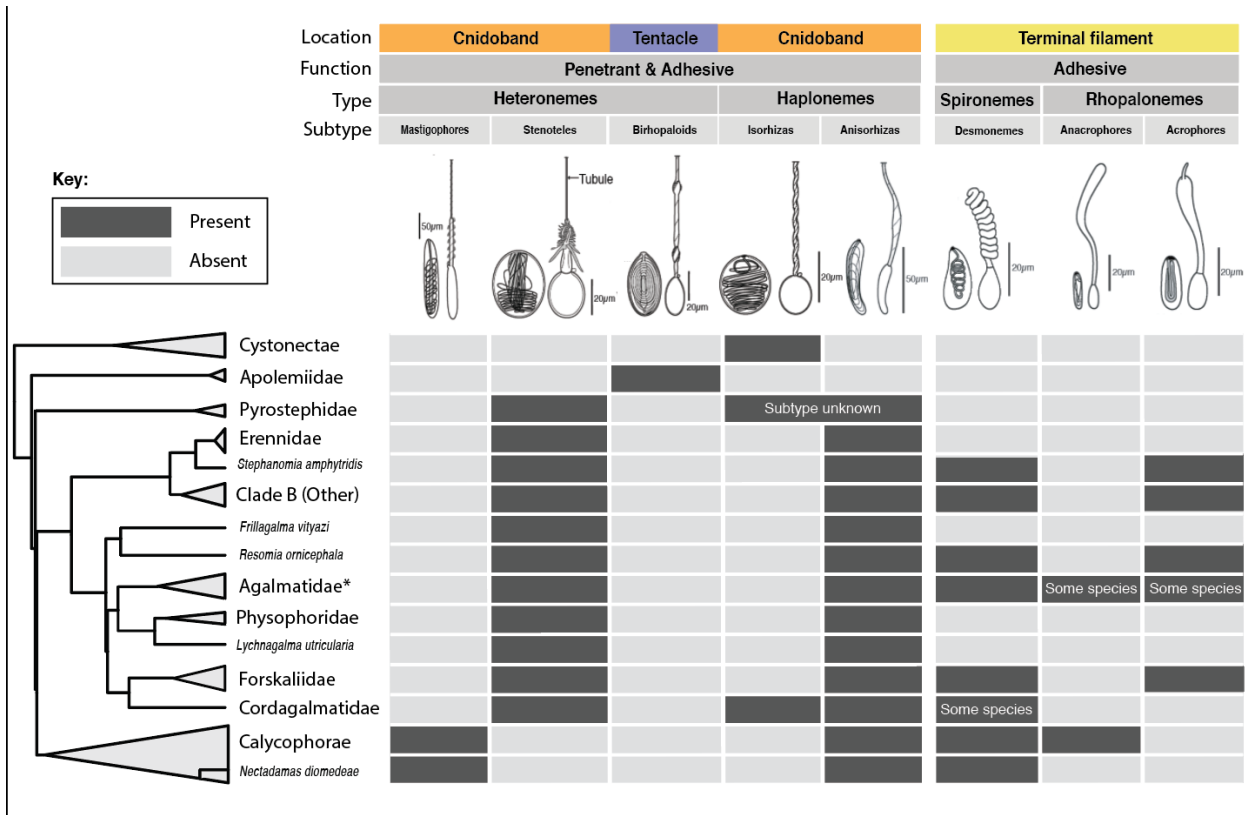


Figure 3: Phylogenetic distribution of nematocyst types, subtypes, functions, and locations in the zooid across the major siphonophore clades. Illustrations reproduced with permission from Mapstone (2014). Undischarged capsules to the left, discharged to the right. Agalmatidae\* here refers only to the genera *Agalma*, *Athorybia*, *Halistemma*, and *Nanomia*.

74 Distantly related organisms that evolved to feed on similar resources often evolve similar  
75 adaptations (Winemiller *et al.*, 2015). In Damian-Serrano *et al.* (2020), we found strong  
76 associations between piscivory and haploneme shape across distantly related siphonophore  
77 lineages. These associations could have been produced by convergent changes in the adaptive  
78 optima of these characters. Here we set out to test this hypothesis using comparative  
79 model fitting methods. Analyzing the diversity of morphological states from a phylogenetic  
80 perspective allows us to identify the specific evolutionary processes that gave rise to it. Here  
81 we fit and compare a variety of macroevolutionary models to siphonophore tentilla morphology  
82 measurement data to identify instances of neutral divergence, stabilizing selection, changes in  
83 the speed of evolution, and convergent evolution.

84 In Damian-Serrano *et al.* (2020) we fit discriminant analyses to identify characters that are  
85 predictive of feeding guild. These discriminant analyses can be used to generate hypotheses  
86 on the diets of ecologically understudied siphonophore species for which we have morphology  
87 data. Here we present a Bayesian prediction for the feeding guild of 45 species using the  
88 discriminant functions and morphological dataset in Damian-Serrano *et al.* (2020). As  
89 mentioned above, tentilla are far from being ornamental shapes and are in fact violently  
90 reactive weapons for prey capture (Mackie *et al.*, 1987; Damian-Serrano *et al.*, 2020). While  
91 we now have detailed characterizations of tentilla morphologies across many species, the  
92 diversity of dynamic performances and their relationships to the undischarged morphologies  
93 have not been examined to date. To address this gap, we set out to record high-speed video  
94 of the *in vivo* discharge dynamics of several siphonophore species at sea, and compare the  
95 kinematic attributes to their morphological characters.

## 96 Methods

97 All character data and the phylogeny analyzed here were published in Damian-Serrano *et al.*  
98 (2020). Details on the specimen collection, microscopy, and measurements can be found in the  
99 aforementioned publication. To facilitate access, we re-included here the character definitions

100 (SM15) and specimen list (SM16) in the Supporting Information. We log-transformed all  
101 the continuous characters that did not pass Shapiro-Wilks normality tests, and used the  
102 ultrametric constrained Bayesian time tree in all comparative analyses. Inapplicable characters  
103 were recorded as NA states, and species with states that could not be measured due to  
104 technical limitations were removed before the analyses. We used the feeding guild categories  
105 detailed in Damian-Serrano *et al.* (2020) with one modification: including all *Forskalia* spp.  
106 as generalists instead of as a single *Forskalia* species on the tree after a reinterpretation  
107 of the data in Purcell (1981). In order to characterize the evolutionary history of tentilla  
108 morphology, we fitted different models generating the observed data distribution given the  
109 phylogeny for each continuous character using the function fitContinuous in the R package  
110 *geiger* (Harmon *et al.*, 2007). These models include a non-phylogenetic white-noise model  
111 (WN), a neutral divergence Brownian Motion model (BM), an early-burst decreasing rate  
112 model (EB), and an Ornstein-Uhlenbeck (OU) model with stabilizing selection around a  
113 fitted optimum trait value. In the same way as Damian-Serrano *et al.* (2020), we then  
114 ordered the models by increasing parametric complexity (WN, BM, EB, OU), and compared  
115 their corrected Akaike Information Criterion (AICc) scores (Sugiura, 1978). We used the  
116 lowest (best) score using a delta cutoff of 2 units to determine significance relative to the next  
117 simplest model (SM10). We calculated model adequacy scores using the R package *arbutus*  
118 (Pennell *et al.*, 2015) (SM11), and calculated phylogenetic signals in each of the measured  
119 characters using Blomberg's K (Blomberg *et al.*, 2003) (SM10). To reconstruct the ancestral  
120 character states of nematocyst types and other categorical traits (character matrix available  
121 in Supplementary Information), we used stochastic character mapping (SIMMAP) using the  
122 package *phytools* (Revell, 2012).

123 In order to examine the degree of phenotypic integration within the tentillum, we explored  
124 the correlational structure among continuous characters and among their evolutionary histories  
125 using principal component analysis (PCA) and phylogenetic PCA (Revell, 2012). Since the  
126 character dataset contains gaps due to missing data and inapplicable character states (SM14),

we carried out these analyses on a subset of species and characters that allowed for the most complete dataset. This was done by removing the terminal filament characters (which are only shared by a small subset of species), and then removing species which had inapplicable states for the remaining characters (apolemiids and cystonects). In addition, we obtained the correlations between the phylogenetic independent contrasts (Felsenstein, 1985) using the package *rphylip* (Revell & Chamberlain, 2014) accounting for intraspecific variation. Using these contrasts, we identified multivariate correlational modules among characters. To test and quantify phenotypic integration between these multivariate modules, we used the phylogenetic phenotypic integration test in the package *geomorph* (Adams *et al.*, 2016).

When comparing the morphospaces of species in different feeding guilds, we carried out a PCA on the complete character dataset while transforming inapplicable states of absent characters to zeros (i.e. cnidoband length = 0 when no cnidoband is present) to account for similarity based on character presence/absence. Using these principal components, we examined the occupation of the morphospace across species in different feeding guilds using a phylogenetic MANOVA with the package *geiger* (Harmon *et al.*, 2007) to assess the variation explained, and a morphological disparity test with the package *geomorph* (Adams *et al.*, 2016) to assess differences in the extent occupied by each guild.

In order to detect and evaluate instances of convergent evolution, we used the package SURFACE (Ingram & Mahler, 2013). This tool identifies OU regimes and their optima given a tree and character data, and then evaluates where the same regime has appeared independently in different lineages. We applied these analyses to the haploneme nematocyst length and width characters as well as to the most complete dataset without inapplicable character states.

In order to generate hypotheses on the diets of siphonophores using tentilla morphology, we used the discriminant analyses of principal components (DAPC) (Jombart *et al.*, 2010) trained in Damian-Serrano *et al.* (2020). We predict the feeding guilds of species in the dataset for which there are no published feeding observations using their morphological data

<sup>154</sup> as inputs, and presenting the predictive output in the form of posterior probabilities for each  
<sup>155</sup> guild category.

<sup>156</sup> In order to observe the discharge behavior of different tentilla, we recorded high speed  
<sup>157</sup> footage (1000-3000 fps) of tentillum and nematocyst discharge by live siphonophore specimens  
<sup>158</sup> (26 species) using a Phantom Miro 320S camera mounted on a stereoscopic microscope. We  
<sup>159</sup> mechanically elicited tentillum and nematocyst discharge using a fine metallic pin. We used  
<sup>160</sup> the Phantom PCC software to analyze the footage. For the 10 species recorded, we measured  
<sup>161</sup> total cnidoband discharge time (ms), heteroneme filament length ( $\mu\text{m}$ ), and discharge speeds  
<sup>162</sup> (mm/s) for cnidoband, heteronemes, haplonemes, and heteroneme shafts when possible (data  
<sup>163</sup> available in the Supplementary Information).

## <sup>164</sup> Results

<sup>165</sup> *Evolutionary history of tentillum morphology* – In Damian-Serrano *et al.* (2020), we produced  
<sup>166</sup> the most speciose siphonophore molecular phylogeny to date, while incorporating the most  
<sup>167</sup> recent findings in siphonophore deep node relationships. This phylogeny revealed for the first  
<sup>168</sup> time that the genus *Erenna* is the sister to *Stephanomia amphytridis*. *Erenna* and *Stephanomia*  
<sup>169</sup> bear the largest tentilla among all siphonophores, thus their monophyly indicates that there  
<sup>170</sup> was a single evolutionary transition to giant tentilla. Siphonophore tentilla range in size  
<sup>171</sup> from  $\sim$ 30  $\mu\text{m}$  in some *Cordagalma* specimens to 2-4 cm in *Erenna* species, and up to 8 cm  
<sup>172</sup> in *Stephanomia amphytridis* (Pugh & Baxter, 2014). Most siphonophore tentilla measure  
<sup>173</sup> between 175 and 1007  $\mu\text{m}$  (1st and 3rd quartiles), with a median of 373  $\mu\text{m}$ . The extreme  
<sup>174</sup> gain of tentillum size in this newly found clade may have important implications for access  
<sup>175</sup> to large prey size classes such as adult deep-sea fishes.

<sup>176</sup> Siphonophore tentilla are defined as lateral, monostichous evaginations of the tentacle  
<sup>177</sup> (including its gastrovascular lumen), armed with epidermal nematocysts (Totton & Bargmann,  
<sup>178</sup> 1965). The buttons on *Physalia* tentacles were not traditionally regarded as tentilla, but  
<sup>179</sup> Bardi & Marques (2007), Munro *et al.* (2018), and our own observations confirm that the

180 buttons contain evaginations of the gastrovascular lumen, thus satisfying all the criteria  
181 for the definition. In this light, and given that most Cystonectae bear conspicuous tentilla,  
182 we conclude (in agreement with Munro *et al.* (2018) and Damian-Serrano *et al.* (2020))  
183 that tentilla were present in the most recent common ancestor of all siphonophores, and  
184 secondarily lost twice, once in *Apolemia* and again in *Bathyphysa conifera*. In order to gain a  
185 broad perspective on the evolutionary history of tentilla, we reconstructed the phylogenetic  
186 positions of the main categorical character shifts (such as gains and losses of nematocyst types)  
187 using stochastic character mapping (SM1-9) and manual reconstructions. This phylogenetic  
188 roadmap of evolutionary novelties is summarized in (Fig. 4).

189 We assume that haploneme nematocysts are ancestrally present in siphonophore tentacles  
190 since they are present in the tentacles of many other hydrozoans (Mariscal, 1974). Haplonemes  
191 are toxin-bearing open-ended nematocysts characterized by the lack of a shaft preceding  
192 the tubule. Two subtypes are found in siphonophores: the isorhizas of homogeneous tubule  
193 width, and the anisorhizas with a slight bulking of the tubule near the base. In Cystonectae,  
194 haplonemes diverged into spherical isorhizas of two size classes. There is one size of haplonemes  
195 in Codonophora, which consist of elongated anisorhizas. Haplonemes were likely lost in the  
196 tentacles of *Apolemia* but retained as spherical isorhizas in other *Apolemia* tissues (Siebert *et*  
197 *al.*, 2013). While heteronemes exist in other tissues of cystonects, they appear in the tentacles  
198 of codonophorans exclusively, as birhopaloids in *Apolemia*, stenoteles in eucladophoran  
199 physonects, and microbasic mastigophores in calycophorans. The four nematocyst types  
200 unique to siphonophores appear in two events in the phylogeny (Fig. 4): birhopaloids arose  
201 in the stem to *Apolemia*, while rhopalonemes (acrophore and anacrophore) and homotrichous  
202 anisorhizas arose in the stem to Tendiculophora.

203 Nematocyst type gain and loss is also associated with prey capture functions. For example,  
204 the loss of desmonemes and rhopalonemes in piscivorous *Erenna*, retaining solely the penetrant  
205 (and venom injecting) anisothizas and stenoteles (two size classes) is reminiscent of the two  
206 size classes of penetrant isorhizas in the fish-specialist cystonects. Moreover, with the gain

207 of anisorhizas, desmonemes, and rhopalonemes, the Tendiculophora gained versatility in  
208 entangling and adhesive functions of the cnidoband and terminal filament, which may have  
209 allowed their feeding niches to diversify. Part of the effectiveness of calycophoran cnidobands  
210 at entangling crustaceans may be attributed to the subspecialization of their heteronemes.  
211 These shifted from the ancestral penetrating stenotele to the microbasic mastigophore (or  
212 eurytele in some species) with a long barbed shaft armed with many long spines. This  
213 heteroneme subtype could be better at interlocking with the setae of crustacean legs and  
214 antennae.

215 In those species that have a functional terminal filament, the desmonemes and  
216 rhopalonemes play a fundamental role in the first stages of adhesion of the prey. In many  
217 species, the tugs of the struggling prey on the terminal filament trigger the cnidoband  
218 discharge (Mackie *et al.*, 1987 and pers. obs.). The adhesive terminal filament has been  
219 lost several times in the Euphysonectae (*Frillagalma*, *Lychnagalma-Physophora*, *Erenna*,  
220 and some species of *Cordagalma*). In these species, we hypothesize that a different trigger  
221 mechanism is at play, possibly involving the prey actively biting or grasping the tentillum or  
222 lure.

223 The clades defined in Damian-Serrano *et al.* (2020) are characterized by unique evolu-  
224 tionary innovations in their tentilla. The clade Eucladophora (containing Pyrostephidae,  
225 Euphysonectae, and Calycophorae) encompasses all of the extant Siphonophore species (178  
226 of 186) except Cystonects and *Apolemia*. Innovations that arose along the stem of this group  
227 include spatially segregated heteroneme and haploneme nematocysts, terminal filaments, and  
228 elastic strands (Fig. 4). Pyrostephids evolved a unique bifurcation of the axial gastrovascular  
229 canal of the tentillum known as the “saccus” (Totton & Bargmann, 1965). The stem to  
230 the clade Tendiculophora (clade containing Euphysonectae and Calycophorae) subsequently  
231 acquired further novelties such as the desmoneme and rhopaloneme (acrophore subtype  
232 ancestral) nematocysts on the terminal filament (Fig. 4), which bears no other nematocyst  
233 type. These are arranged in sets of 2 parallel rhopalonemes for each single desmoneme (Skaer,

<sup>234</sup> 1988, 1991). The involucrum is an expansion of the epidermal layer that can cover part or  
<sup>235</sup> all of the cnidoband (Fig. 2). This structure, together with differentiated larval tentilla,  
<sup>236</sup> appeared in the stem branch to Clade A physonects. Calycophorans evolved novelties such as  
<sup>237</sup> larger desmonemes at the distal end of the cnidoband, pleated pedicles with a “hood” (here  
<sup>238</sup> considered homologous to the involucrum) at the proximal end of the tentillum, anacrophore  
<sup>239</sup> rhopalonemes, and microbasic mastigophore-type heteronemes. While calycophorans have  
<sup>240</sup> diversified into most of the extant described siphonophore species (108 of 186), their tentilla  
<sup>241</sup> have not undergone any major categorical gains or losses since their most recent common  
<sup>242</sup> ancestor. Nonetheless, they have evolved a wide variation in nematocyst and cnidoband  
<sup>243</sup> sizes. Ancestrally (and retained in most prayomorphs and hippopodids), the calycophoran  
<sup>244</sup> tentillum is recurved where the proximal and distal ends of the cnidoband are close together.  
<sup>245</sup> Diphyomorph tentilla are slightly different in shape, with straighter cnidobands.

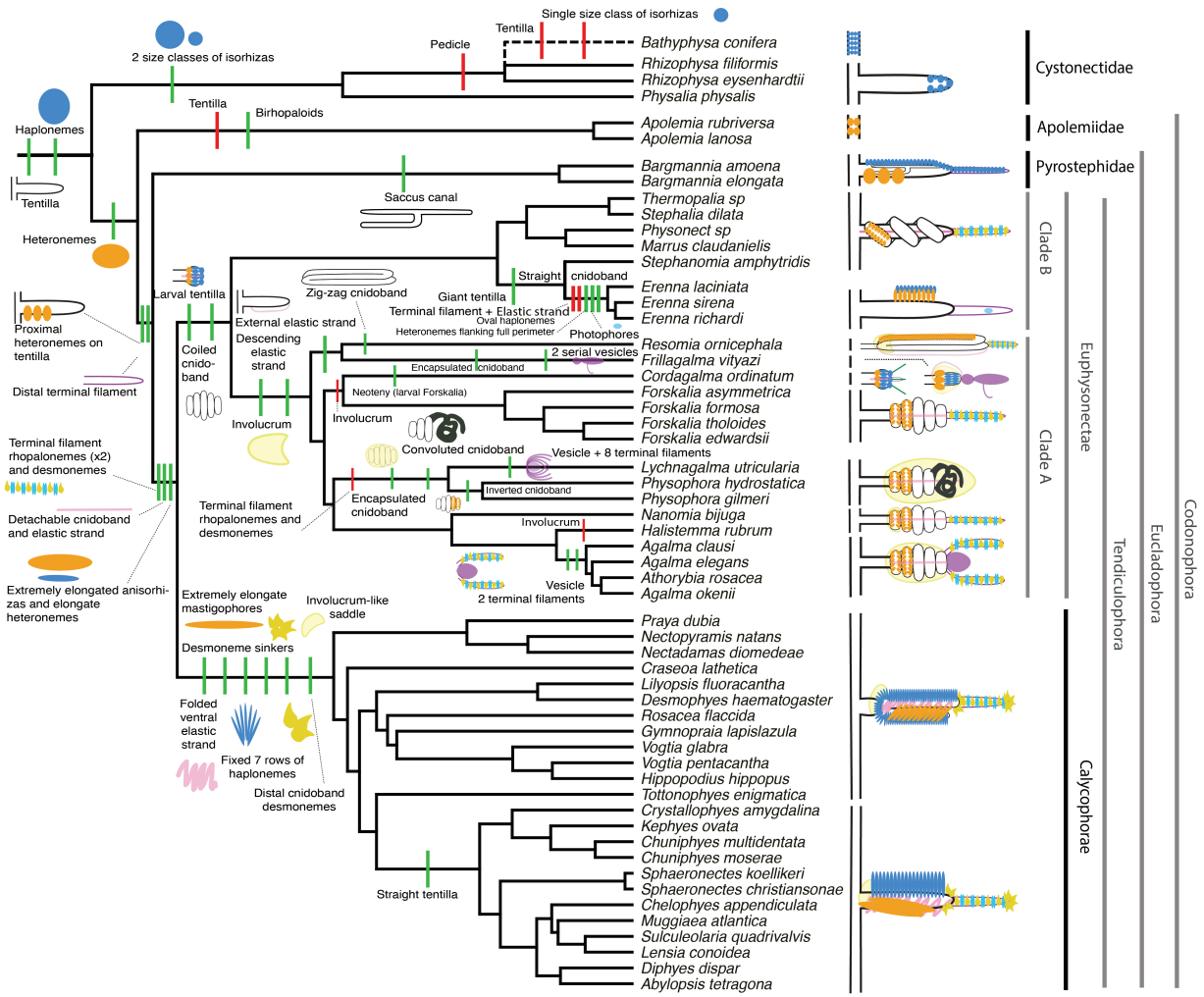


Figure 4: Siphonophore cladogram with the main categorical character gains (green) and losses (red) mapped. Some branch lengths were modified from the Bayesian chronogram to improve readability. The main visually distinguishable tentillum types are sketched next to the species that bear them, showing the location and arrangement of the main characters. In large, complex-shaped euphysonect tentilla, haplonemes were omitted for simplification. The hypothesized phylogenetic placement of the rhizophysid *Bathyphysa conifera*, for which no molecular data are yet available, was added manually (dashed line).

*Evolution of tentillum and nematocyst characters* – Most (74%) characters present a significant phylogenetic signal, yet only total nematocyst volume, haploneme length, and heteroneme-to-cnidoband length ratio had a phylogenetic signal with K larger than 1 (SM10). Total nematocyst volume and cnidoband-to-heteroneme length ratio showed strongly conserved phylogenetic signals. The majority (67%) of characters were best fitted by BM models, indicating a history of neutral constant divergence. We did not find any relationship between phylogenetic signal and specific model support, where characters with high and low phylogenetic signal were broadly distributed among the best fitted for each model. One-third of the characters measured in Damian-Serrano *et al.* (2020) did not recover significant support for any of the phylogenetic models tested, indicating they are either not phylogenetically conserved, or they evolved under a complex evolutionary process not represented among the models tested (SM10). Haploneme nematocyst length was the only character with support for an EB model of decreasing rate of evolution with time. No character had support for a single-optimum OU model (when not informed by feeding guild regime priors). The model adequacy tests (SM11) indicate that many characters may have a relationship between the states and the rates of evolution (Sasr) not captured in the basic models compared here, accompanied by a signal of unaccounted rate heterogeneity (Cvar). No characters show significant deviations in the overall rate of evolution estimated (Msig). Some characters show a perfect fit (no significant deviations across all metrics) under BM evolution, such as heteroneme shape, length, width & volume, haploneme width & SA/V, tentacle width and pedicle width. Haploneme row number and rhopaloneme shape have significant deviations across four metrics, indicating that BM (best model) is a poor fit. These characters likely evolved under complex models which would require many more data points than we have available to fit with accuracy.

*Phenotypic integration of the tentillum* – Phenotypically integrated structures maintain evolutionary correlations between its constituent characters. Of the phylogenetic correlations among tentillum and nematocyst characters examined here (Fig. 5a, lower triangle), 81.3%

were positive and 18.7% were negative, while of the ordinary correlations (Fig. 5a, upper triangle) 74.6% were positive and 25.4% were negative. Half (49.9%) of phylogenetic correlations were  $>0.5$ , while only 3.6% are  $< -0.5$ . Similarly, among the correlations across extant species, 49.1% were  $>0.5$  and only 1.5% were  $< -0.5$ . In addition, we found that 13.9% of character pairs had opposing phylogenetic and ordinary correlation coefficients (Fig. 5B). Just 4% of character pairs have negative phylogenetic and positive ordinary correlations (such as rhopaloneme elongation  $\sim$  heteroneme-to-cnidoband length ratio and haploneme elongation, or haploneme elongation  $\sim$  heteroneme number), and only 9.9% of character pairs had positive phylogenetic correlation yet negative ordinary correlation (such as heteroneme elongation  $\sim$  cnidoband convolution and involucrum length, or rhopaloneme elongation with cnidoband length). These disparities could be explained by Simpson's paradox (Blyth, 1972): the reversal of the sign of a relationship when a third variable (or a phylogenetic topology, as suggested by Uyeda *et al.* (2018)) is considered. However, no character pair had correlation coefficient differences larger than 0.64 between ordinary and phylogenetic correlations (heteroneme shaft extension  $\sim$  rhopaloneme elongation has a Pearson's correlation of 0.10 and a phylogenetic correlation of -0.54). Rhopaloneme elongation shows the most incongruencies between phylogenetic and ordinary correlations with other characters. We identified four hypothetical modules among the tentillum characters: (1) The tentillum scaffold module including cnidoband length & width, nematocyst row number, pedicle & elastic strand width, tentacle width; (2) the heteroneme module including heteroneme length & width, shafts length & width; (3) the haploneme module including length and width; and (4) the terminal filament module including desmoneme & rhopaloneme length & width. The phenotypic integration test showed significant integration signal between all modules, tentillum and haploneme modules sharing the greatest regression coefficient (SM12).

*Evolution of nematocyst shape* – The greatest evolutionary change in haploneme nematocyst shape occurred in a single shift towards elongation in the stem of Tendiculophora, which contains the majority of described siphonophore species, *i.e.* all siphonophores other

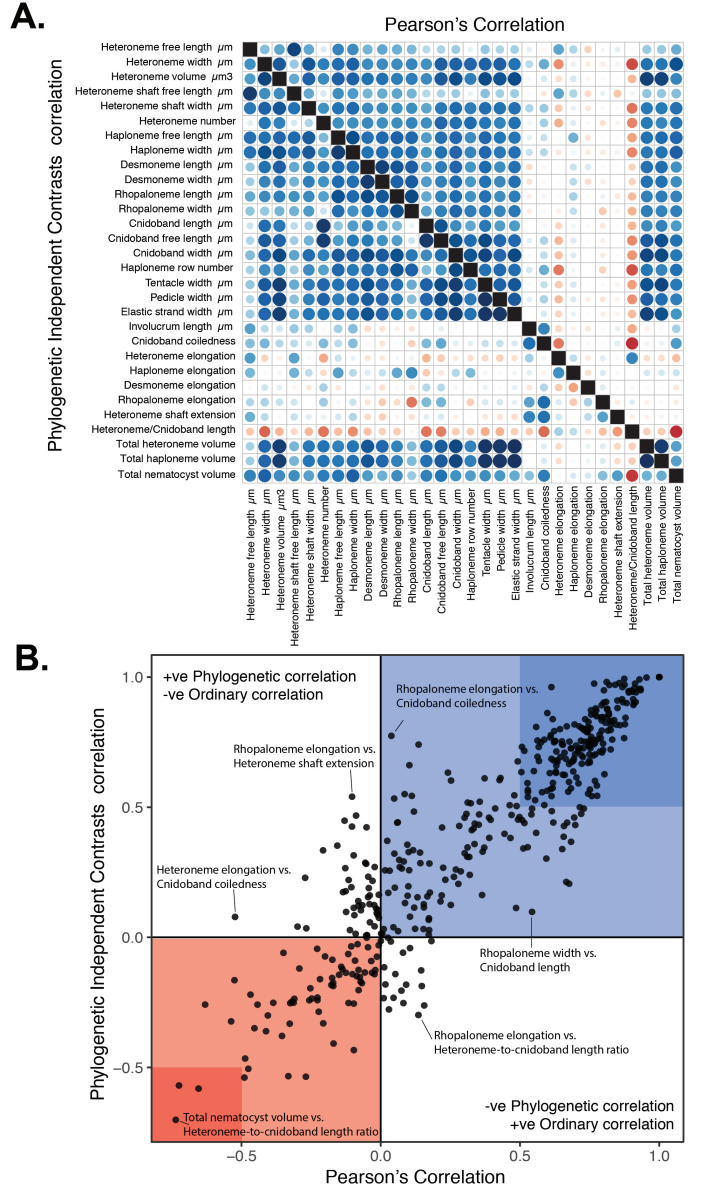


Figure 5: A. Correlogram showing strength of ordinary (upper triangle) and phylogenetic (lower triangle) correlations between characters. Both size and color of the circles indicate the strength of the correlation ( $R^2$ ). B. Scatterplot of phylogenetic correlation against ordinary correlation showing a strong linear relationship ( $R^2 = 0.92$ , 95% confidence between 0.90 and 0.93). Light red and blue boxes indicate congruent negative and positive correlations respectively. Darker red and blue boxes indicate strong ( $<-0.5$  or  $>0.5$ ) negative and positive correlation coefficients respectively.

<sup>300</sup> than Cystonects, *Apolemia*, and Pyrostephidae. There is one secondary return to more  
<sup>301</sup> oval, less elongated haplonemes in *Erenna*, but it does not reach the sphericity present  
<sup>302</sup> in Cystonectae or Pyrostephidae (Fig. 6). Heteroneme evolution presents a less discrete  
<sup>303</sup> evolutionary history. Tendiculophora evolved more elongate heteronemes along the stem, but  
<sup>304</sup> the difference between theirs and other siphonophores' is much smaller than the variation  
<sup>305</sup> in shape within Tendiculophora, bearing no phylogenetic signal within this clade. In this  
<sup>306</sup> clade, the evolution of heteroneme shape has diverged in both directions, and there is no  
<sup>307</sup> correlation with haploneme shape (Fig. 6), which has remained fairly constant (elongation  
<sup>308</sup> between 1.5 and 2.5).

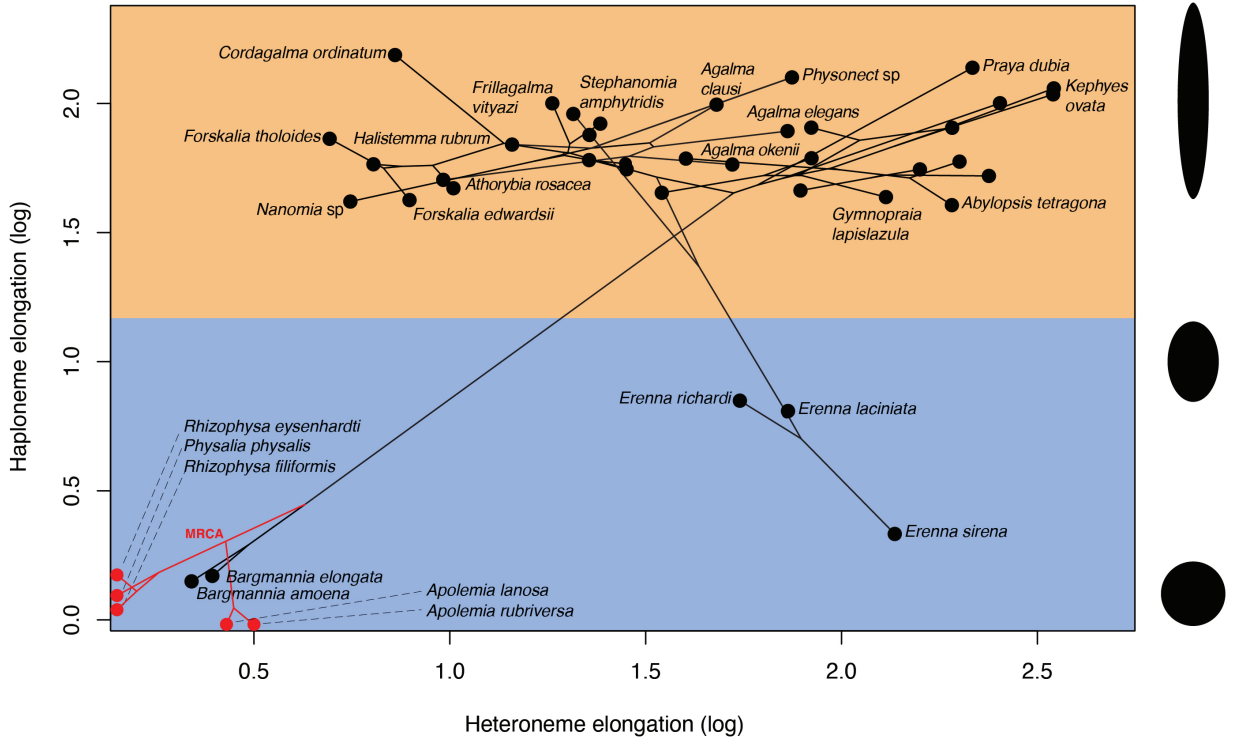


Figure 6: Phylomorphospace showing haploneme and heteroneme elongation (log scaled). Orange area delimits rod-shaped haplonemes, the blue area covers oval and round-shaped haplonemes. Smaller dots and lines represent phylogenetic relationships and ancestral states of internal nodes under BM. Species nodes in red lack either haplonemes or heteronemes, and their values are projected onto the axis of the nematocyst type they bear. Cystonects have no tentacle heteronemes and are projected onto the haploneme axis. Apolemiids have no tentacle haplonemes and are projected onto the heteroneme axis.

309 Haploneme and heteroneme shape share 21% of their variance across extant values, and  
310 53% of the variance in their shifts along the branches of the phylogeny. However, much of  
311 this correlation is due to the sharp contrast between Pyrostephidae and their sister group  
312 Tendiculophora. We searched for regime shifts in the evolution of haploneme nematocyst  
313 shape characters using SURFACE (Ingram & Mahler, 2013). SURFACE identified eight  
314 distinct OU regimes in the evolutionary history of haploneme length and width (Fig. 7A).  
315 The different regimes are located (1) in cystonects, (2) in most of Tendiculophora, (3) in  
316 most diphymorphs, (4) in *Cordagalma ordinatum*, (5) in *Stephanomia amphytridis*, (6) in  
317 pyrostephids, (7) in *Diphyes dispar* + *Abylopsis tetragona*, and (8) in *Erenna* spp.

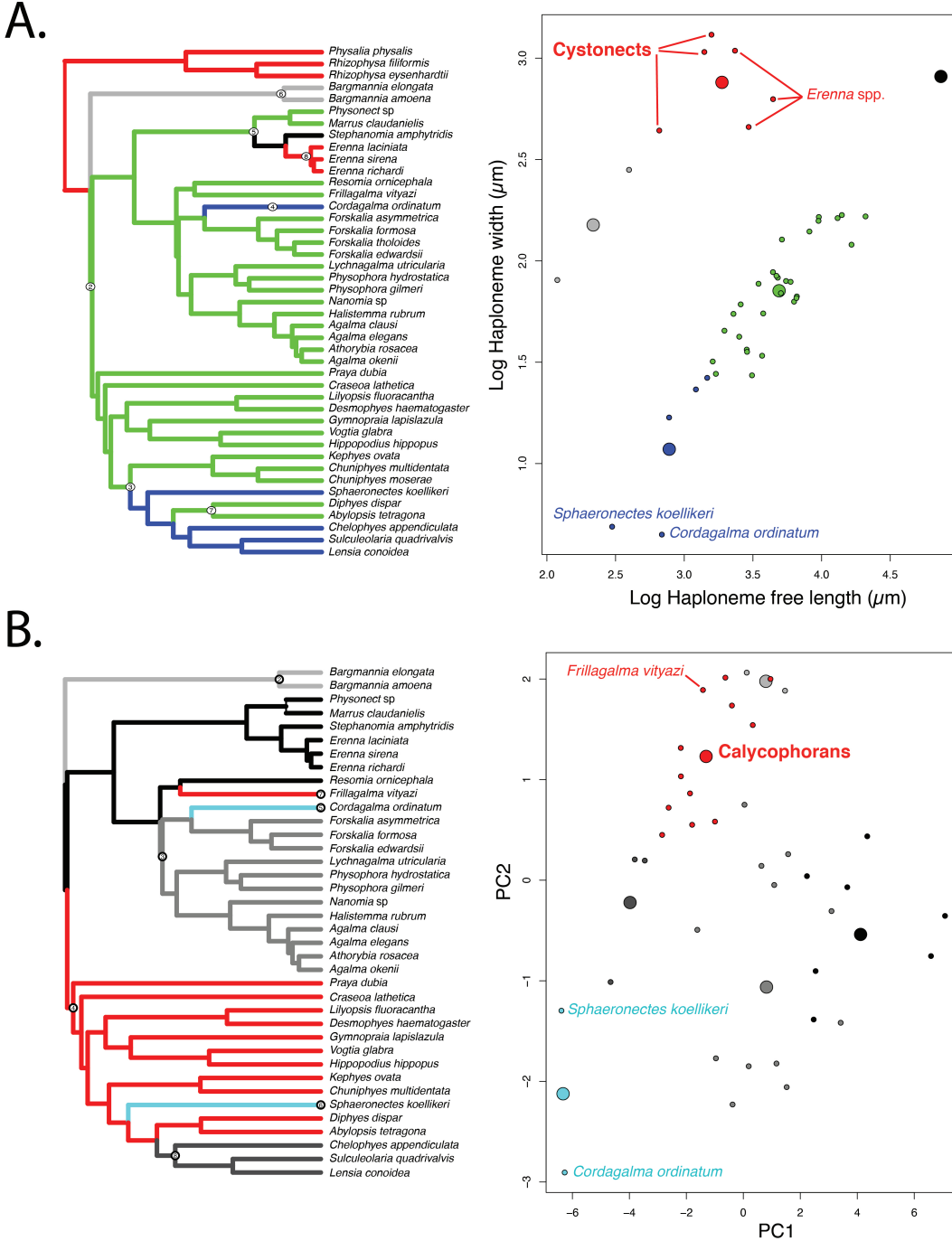


Figure 7: SURFACE plots showing convergent evolutionary regimes modelled under OU for (A) haploneme nematocyst length & width, and (B) for PC1 & PC2 of all continuous characters with the exception of terminal filament nematocysts, and removing taxa with inapplicable character states. Node numbers on the tree label different regimes, regimes of the same color are identified as convergent. Small circles on the scatterplots indicate species values, large circles indicate the average position of the OU optima ( $\theta$ ) for a given combination of convergent regimes.

<sup>318</sup> In the non-phylogenetic PCA morphospace using only characters derived from simple  
<sup>319</sup> measurements (Fig. 8), PC1 (aligned with tentillum and tentacle size) explained 69.3% of  
<sup>320</sup> the variation in the tentillum morphospace, whereas PC2 (aligned with heteroneme length,  
<sup>321</sup> heteroneme number, and haploneme arrangement) explained 13.5%. In a phylogenetic PCA,  
<sup>322</sup> 63% of the evolutionary variation in the morphospace is explained by PC1 (aligned with  
<sup>323</sup> shifts in tentillum size), while 18% is explained by PC2 (aligned with shifts in heteroneme  
<sup>324</sup> number and involucrum length).

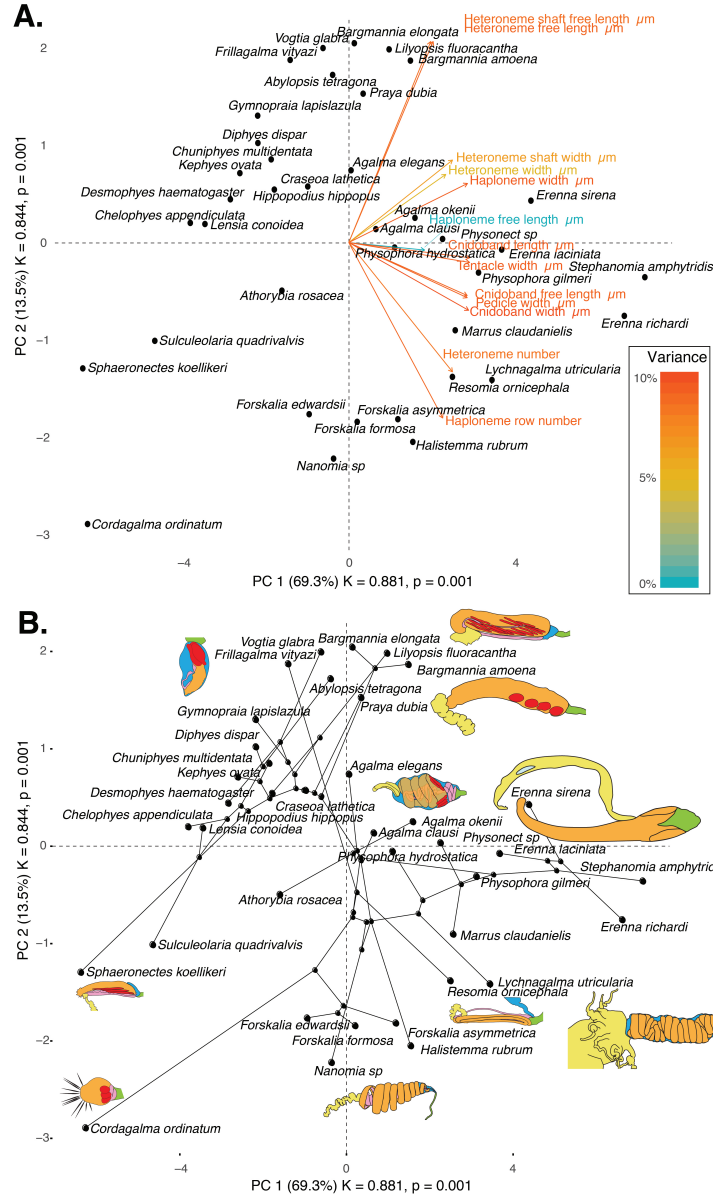


Figure 8: PCA of the simple-measurement continuous characters principal components, excluding ratios and composite characters. A. Variance explained by each variable in the PC1-PC2 plane. Axis labels include the phylogenetic signal (K) for each component and p-value. B. Phylogenetic relationships between the species points and reconstructed ancestors distributed in that same space.

325        *Morphospace occupation* – In order to examine the occupation structure of the morphospace  
326 across all siphonophore species in the dataset, we cast a PCA on the data after transforming  
327 inapplicable states (due to absence of character) to zeroes. This allows us to accommodate  
328 species with many missing characters (such as cystonects or apolemiids), and to account  
329 for common absences as morphological similarities. In this ordination, PC1 (aligned with  
330 cnidoband size) explains 47.45% of variation and PC2 (aligned with heteroneme volume  
331 and involucrum length) explains 16.73% of variation. When superimposing feeding guilds  
332 onto the morphospace (Fig. 9), we find that the morphospaces of each feeding guild are  
333 only slightly overlapping in PC1 and PC2. A phylogenetic MANOVA showed that feeding  
334 guilds explain 27.63% of variance across extant species ( $p$  value < 0.000001), and 20.97%  
335 of the variance when accounting for phylogeny, an outcome significantly distinct from the  
336 expectation under neutral evolution ( $p$ -value = 0.0196). In addition, a morphological disparity  
337 analysis accounting for phylogenetic structure shows that the morphospace of fish specialists  
338 is significantly broader than that of generalists and other specialists. This is due to the large  
339 morphological disparities between cystonects and piscivorous euphysonects. There are no  
340 significant differences among the morphospace disparities of the other feeding guilds.

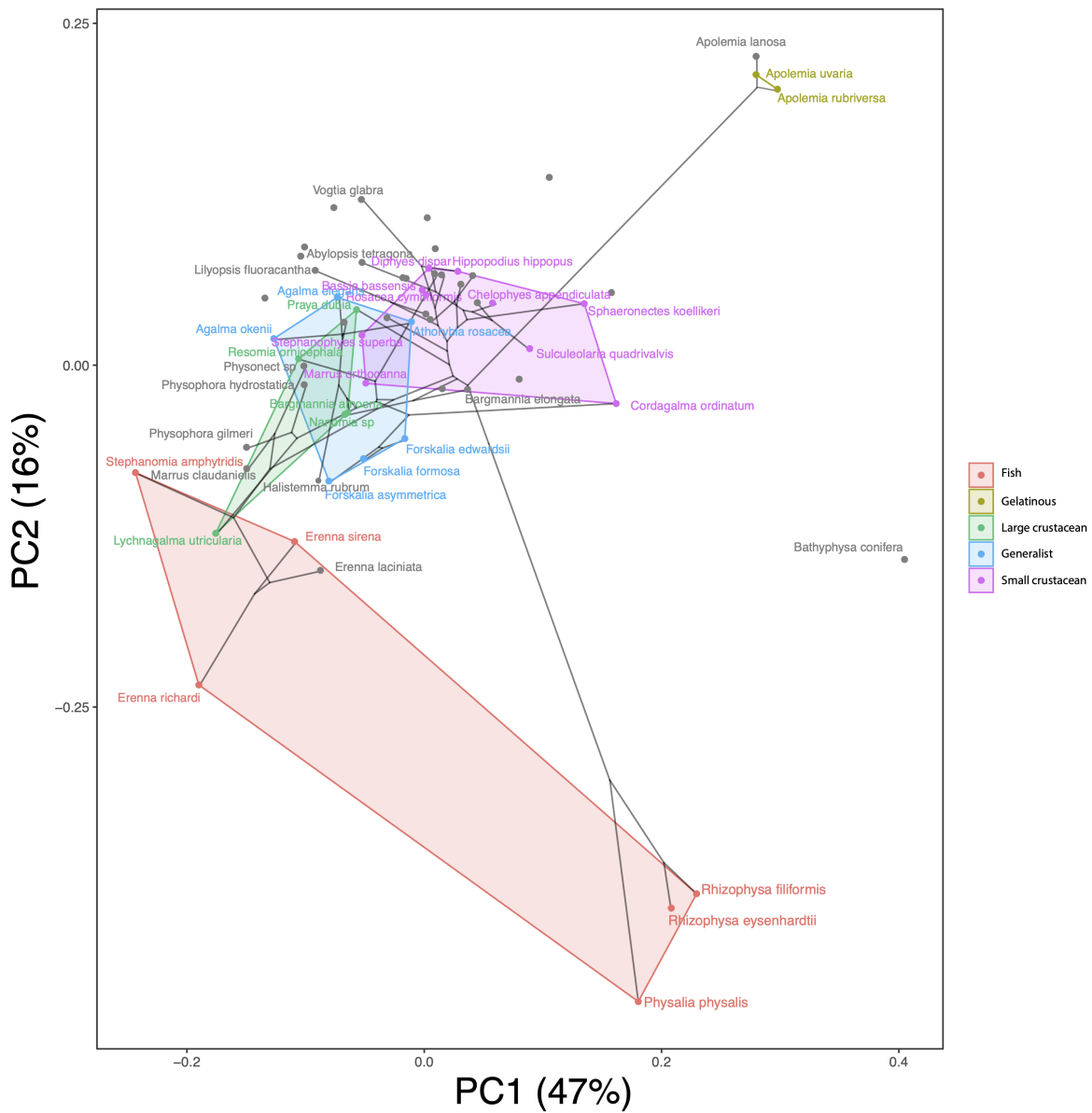


Figure 9: Phylomorphospace showing PC1 and PC2 from a PCA of continuous morphological characters with inapplicable states transformed to zeroes, overlapped with polygons conservatively defining the space occupied by each feeding guild. Lines between species coordinates show the phylogenetic relationships between them.

*Convergent evolution* – Convergence is a widespread evolutionary phenomenon where distantly related clades independently evolve similar phenotypes. When the dimensionality of the state space is small as it is in tentilla morphology, convergence is more likely given the same amount of evolutionary change. Using the package SURFACE (Ingram & Mahler, 2013), we identified convergence in haploneme nematocyst shape and in morphospace position. In Damian-Serrano *et al.* (2020), we identified haploneme nematocyst shape as one of the traits associated with the convergent evolution of piscivory. Here we find that indeed wider haploneme nematocysts have convergently evolved in the piscivore cytonects and *Erenna* spp. (Fig. 7A). Extremely narrow haplonemes have also evolved convergently in *Cordagalma ordinatum* and copepod specialist calycophorans such as *Sphaeronectes koellikeri*. When integrating many traits into a couple principal components, we find two distinct convergences between euphysonects and calycophorans with a reduced prey capture apparatus. Those convergences are between *Frillagalma vityazi* and calycophorans, and once again between *Cordagalma ordinatum* and *Sphaeronectes koellikeri* (Fig. 7B).

*Functional morphology of tentillum and nematocyst discharge* – Tentillum and nematocyst discharge high speed videos and measurements are available in the Supplementary Information. While the sample sizes of these measurements were insufficient to draw reliable statistical results at a phylogenetic level, we did observe patterns that may be relevant to their functional morphology. For example, cnidoband length is strongly correlated with discharge speed ( $p$  value = 0.0002). This explains much of the considerable difference between euphysonect and calycophoran tentilla discharge speeds (average discharge speeds: 225.0mm/s and 41.8mm/s respectively; t-test  $p$  value = 0.011), since the euphysonects have larger tentilla than the calycophorans among the species recorded. In addition, we observed that calycophoran haploneme tubules fire faster than those of euphysonects (t-test  $p$  value = 0.001). Haploneme nematocysts discharge 2.8x faster than heteroneme nematocysts (t-test  $p$  value = 0.0012). Finally, we observed that the stenoteles of the Euphysonectae discharge a helical filament that “drills” itself through the medium it penetrates as it everts.

*Generating dietary hypotheses using tentillum morphology* – For many siphonophore species, no feeding observations have yet been published. To help bridge this gap of knowledge, we generated hypotheses about the diets of these understudied siphonophores (Fig. 10) based on their known tentacle morphology using one of the linear discriminant analyses of principal components (DAPC) fitted in Damian-Serrano *et al.* (2020). This provides concrete predictions to be tested in future work and helps extrapolate our findings to many poorly known species that are extremely difficult to collect and observe. The discriminant analysis for feeding guild (7 principal components, 4 discriminants) produced 100% discrimination, and the highest loading contributions were found for the characters (ordered from highest to lowest): Involucrum length, heteroneme volume, heteroneme number, total heteroneme volume, tentacle width, heteroneme length, total nematocyst volume, and heteroneme width. We used the predictions from this discriminant function to generate hypotheses about the feeding guild of 45 species in the morphological dataset. This extrapolation predicts that two other *Apolemia* species are gelatinous prey specialists like *Apolemia rubriversa*, and predicts that *Erenna laciniata* is a fish specialist like *Erenna richardi*. When predicting soft- and hard-bodied prey specialization, the DAPC achieved 90.9% discrimination success, only marginally confounding hard-bodied specialists with generalists (SM13). The main characters driving this discrimination are involucrum length, heteroneme number, heteroneme volume, tentacle width, total nematocyst volume, total haploneme volume, elastic strand width, and heteroneme length.

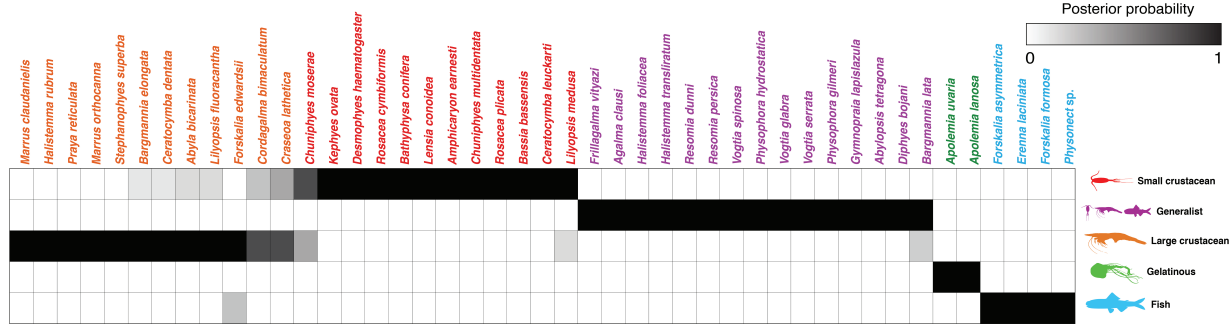


Figure 10: Hypothetical feeding guilds for siphonophore species predicted by a 6 PCA DAPC. Cell darkness indicates the posterior probability of belonging to each guild. The training dataset was transformed so inapplicable states are computed as zeroes. Species are sorted and colored according to their predicted feeding guild.

## 388 Discussion

389 *On the evolution of tentilla morphology* – The evolutionary history of siphonophore tentilla  
 390 shows three major transition points which have structured the morphological diversity we  
 391 see today. First, the earliest split between codonophorans and cystonects divides lineages  
 392 with penetrating isorhizas from those which utilize heteronemes for prey capture. Second,  
 393 the split between apolemiids and eucladophorans divided the simple-tentacled *Apolemia* from  
 394 the lineage that evolved composite tentilla with heteronemes and haplonemes. Finally, the  
 395 branch leading to tendiculophorans fostered innovations such as the elastic strands and the  
 396 terminal filament nematocysts which produced the most complex tentilla structures and  
 397 greatest morphological diversity we observe among siphonophores.

398 Siphonophore tentilla are beautifully complex and highly diverse. Our new analyses  
 399 show, however, that the siphonophore tentillum morphospace actually has a fairly low extant  
 400 dimensionality due to having an evolutionary history with many synchronous, correlated  
 401 changes. This can be due to many causes including structural constraints, developmental  
 402 constraints, or selection that reduces the viable state space. Though siphonophore development  
 403 has not been extensively studied, what is known suggests that developmental constraints alone  
 404 could not explain the highly correlated evolutionary changes we observe. The nematocysts  
 405 that arm the tentillum are developed in a completely separate region of the gastrozooid

406 (Carré, 1972) and then migrate and assemble within the tentillum later on (Skaer, 1988).  
407 This lack of proximity and physical independence of development between traits makes  
408 developmental constraints unlikely. Surprisingly, many of the strong correlations we find  
409 are between nematocyst and structural tentillum characters. Therefore, we hypothesize the  
410 genetic correlations and phenotypic integration between tentillum and nematocyst characters  
411 are maintained through natural selection on separate regulatory networks, out of the necessity  
412 to work together and meet the spatial, mechanical, and functional constraints of their prey  
413 capture behavior. In order to adequately test these hypotheses, future work would need to  
414 study the genetic mechanisms underlying the development of tentilla from a comparative,  
415 evolutionary approach. Fortunately, the unique biology of siphonophore tentacles displays  
416 the full developmental sequence of tentilla along each tentacle, making siphonophores an  
417 ideal system for the comparative study of development.

418 In Damian-Serrano *et al.* (2020) we examined the covariance terms in the multivariate rate  
419 matrix for the evolution of tentillum and nematocyst characters. Building on this work, here  
420 we examine the correlations among the trait values while accounting for phylogenetic structure.  
421 The results for both analyses indicate that tentilla are not only phenotypically integrated (with  
422 widespread evolutionary correlations across structures) but also show patterns of evolutionary  
423 modularity, where different sets of characters appear to evolve in stronger correlations among  
424 each other than with other characters (Wagner, 1996). This may be indicative of the  
425 underlying genetic and developmental dependencies among closely homologous nematocyst  
426 types (such as desmonemes and rhopalonemes) and structures. In addition, these evolutionary  
427 modules point to hypothetical functional modules. For example, the coiling degree of the  
428 cnidoband and the extent of the involucrum have correlated rates of evolution, while the  
429 involucrum may help direct the whiplash of the uncoiling cnidoband distally (towards the  
430 prey). The evolutionary innovation of the Tendiculophora tentilla with shooting cnidobands  
431 and modular regions may have facilitated further dietary diversification. A specific instance  
432 of this dietary diversification may have been the access to the abundant small crustacean

433 prey such as copepods. The rapid darting escape response of copepods may preclude their  
434 capture in siphonophores without shooting cnidobands. The trophic opportunities unlocked  
435 by these morphological novelties may be responsible for the far greater number of species in  
436 Tendicilophora than its relatives Cystonectae, Apolemiidae, and Pyrostephidae.

437 *Heterochrony and convergence in the evolution of tentilla with diet* - In addition to identi-  
438 fying shifts in prey type, Damian-Serrano *et al.* (2020) revealed the specific morphological  
439 changes in the prey capture apparatus associated with these shifts. Copepod-specialized  
440 diets have evolved independently in *Cordagalma* and some calycophorans. These evolutionary  
441 transitions happened together with transitions to smaller tentilla with fewer and smaller  
442 cnidoband nematocysts. We found that these morphological transitions evolved convergently  
443 in these taxa. Tentilla are expensive single-use structures (Mackie *et al.*, 1987), therefore we  
444 would expect that specialization in small prey would beget reductions in the size of the prey  
445 capture apparatus to the minimum required for the ecological performance. Such a reduction  
446 in size would require extremely fast rates of trait evolution in an ordinary scenario. However,  
447 *Cordagalma*'s tentilla strongly resemble the larval tentilla (only found in the first-budded  
448 feeding body of the colony) of their sister genus *Forskalia*. This indicates that the evolution of  
449 *Cordagalma* tentilla could be a case of paedomorphic heterochrony associated with predatory  
450 specialization on smaller prey. This developmental shift may have provided a shortcut for  
451 the evolution of a smaller prey capture apparatus.

452 Our work identifies yet another novel example of convergent evolution. The region of the  
453 tentillum morphospace occupied by calycophorans was independently (and more recently)  
454 occupied by the physonect *Frillagalma vityazi* (Fig. 7B). Like calycophorans, *Frillagalma*  
455 tentilla have small C-shaped cnidobands with a few rows of anisorhizas. Unlike calycophorans,  
456 they lack paired elongate microbasic mastigophores. Instead, they bear exactly three oval  
457 stenoteles, and their cnidobands are followed by a branched vesicle, unique to this genus.  
458 Their tentillum morphology is very different from that of other related physonects, which tend  
459 to have long, coiled, cnidobands with many paired oval stenoteles. Our SURFACE analysis

460 clearly indicates a regime convergence in the cnidoband morphospace between *Frillagalma* and  
461 calycophorans (Fig. 7B). Most studies on calycophoran diets have reported their prey to be  
462 primarily composed of small crustaceans, such as copepods or ostracods (Purcell, 1981, 1984).  
463 The diet of *Frillagalma vityazi* is unknown, but this morphological convergence suggests that  
464 they evolved to capture similar kinds of prey. However, our DAPCs predict that *Frillagalma*  
465 has a generalist niche (Fig. 10) with both soft and hard-bodied prey (SM13).

466 *Evolution of nematocyst shape* – A remarkable feature of siphonophore haplonemes is  
467 that they are outliers to all other Medusozoa in their surface area to volume relationships,  
468 deviating significantly from sphericity (Thomason, 1988). This suggests a different mechanism  
469 for their discharge that could be more reliant on capsule tension than on osmotic potentials  
470 (Carré & Carré, 1980), and strong selection for efficient nematocyst packing in the cnidoband  
471 (Thomason, 1988; Skaer, 1988). Our results show that Codonophora underwent a shift  
472 towards elongation and Cystonectae towards sphericity, assuming the common ancestor had  
473 an intermediate state. Since we know that the haplonemes of other hydrozoan outgroups are  
474 generally spheroid, it is more parsimonious to assume that cystonects are simply retaining  
475 this ancestral state. Later, we observe a return to more rounded (ancestral) haplonemes in  
476 *Erenna*, concurrent with a secondary gain of a piscivorous trophic niche, like that exhibited  
477 by cystonects. Our SURFACE analysis shows that this transition to roundness is convergent  
478 with the regime occupied by cystonects (Fig. 7A). Purcell (1984) showed that haplonemes  
479 have a penetrating function as isorhizas in cystonects and an adhesive function as anisorhizas  
480 in Tendiculophora. It is no coincidence that the two clades that have converged to feed  
481 primarily on fish have also converged morphologically toward more compact haplonemes.  
482 Isorhizas in cystonects are known to penetrate the skin of fish during prey capture, and to  
483 deliver the toxins that aid in paralysis and digestion (Hessinger, 1988). *Erenna*'s anisorhizas  
484 are also able to penetrate human skin and deliver a painful sting (Pugh, 2001), a common  
485 feature of piscivorous cnidarians like the Portuguese man-o-war or box jellies.

486 The implications of these results for the evolution of nematocyst function are that

487 an innovation in the discharge mechanism of haplonemes may have occurred during the  
488 main shift to elongation. Elongate nematocysts can be tightly packed into cnidobands.  
489 We hypothesize this may be a Tendiculophora lineage-specific adaptation to packing more  
490 nematocysts into a limited tentillum space, as suggested by (Skaer, 1988). Thomason  
491 (1988) hypothesized that smaller, more spherical nematocysts, with a lower surface area  
492 to volume ratio, are more efficient in osmotic-driven discharge and thus have more power  
493 for skin penetration. The elongated haplonemes of crustacean-eating Tendiculophora have  
494 never been observed penetrating their crustacean prey (Purcell, 1984), and are hypothesized  
495 to entangle the prey through adhesion of the abundant spines to the exoskeletal surfaces  
496 and appendages. Entangling requires less acceleration and power during discharge than  
497 penetration, as it does not rely on point pressure. In fish-eating cystonects and *Erenna* species,  
498 the haplonemes are much less elongated and very effective at penetration, in congruence with  
499 the osmotic discharge hypothesis. Tendiculophora, composed of the clades Euphysonectae  
500 and Calycophorae, includes the majority of siphonophore species. Within these clades are the  
501 most abundant siphonophore species, and a greater morphological and ecological diversity is  
502 found. We hypothesize that this packing-efficient haploneme morphology may have also been  
503 a key innovation leading to the diversification of this clade. However, other characters that  
504 shifted concurrently in the stem of this clade could have been equally responsible for their  
505 extant diversity.

506 *Generating hypotheses on siphonophore feeding ecology* – One motivation for our research  
507 is to understand the links between prey-capture tools and diets so we can generate hypotheses  
508 about the diets of predators based on morphological characteristics. Indeed, our discriminant  
509 analyses were able to distinguish between different siphonophore diets based on morphological  
510 characters alone. The models produced by these analyses generated testable predictions  
511 about the diets of many species for which we only have morphological data of their tenta-  
512 cles. For example, the unique tentilla morphology of *Frillagalma* is predicted to render a  
513 generalist diet, or one of the undescribed deep-sea physonect species examined is predicted

514 to be a fish specialist, which is congruent with its close phylogenetic relationship to other  
515 piscivorous physonects. While the limited dataset used here is informative for generating  
516 tentative hypotheses, the empirical dietary data are still scarce and insufficient to cast robust  
517 predictions. This reveals the need to extensively characterize siphonophore diets and feeding  
518 habits. In future work, we will test these ecological hypotheses and validate these models  
519 by directly characterizing the diets of some of those siphonophore species. Predicting diet  
520 using morphology is a powerful tool to reconstruct food web topologies from community  
521 composition alone. In many of the ecological models found in the literature, interactions  
522 among the oceanic zooplankton have been treated as a black box (Mitra, 2009). The ability  
523 to predict such interactions, including those of siphonophores and their prey, will enhance  
524 the taxonomic resolution of nutrient-flow models constructed from plankton community  
525 composition data.

## 526 Acknowledgements

527 This work was supported by the Society of Systematic Biologists (Graduate Student Award  
528 to A.D.S.); the Yale Institute of Biospheric Studies (Doctoral Pilot Grant to A.D.S.); and  
529 the National Science Foundation (Waterman Award to C.W.D., OCE-1829835 to C.W.D.,  
530 OCE-1829805 to S.H.D.H., and OCE-1829812 to C. Anela Choy). A.D.S. was supported by  
531 a Fulbright Spain Graduate Studies Scholarship.

532 **References**

- 533 Adams, D.C., Collyer, M., Kaliontzopoulou, A., & Sherratt, E. (2016). Geomorph: Software  
534 for geometric morphometric analyses.
- 535 Bardi, J. & Marques, A.C. (2007). Taxonomic redescription of the portuguese man-of-war,  
536 physalia physalis (cnidaria, hydrozoa, siphonophorae, cystonectae) from brazil. *Iheringia.*  
537 *Série Zoologia*, 97, 425–433.
- 538 Blomberg, S.P., Garland, T., & Ives, A.R. (2003). Testing for phylogenetic signal in  
539 comparative data: Behavioral traits are more labile. *Evolution*, 57, 717–745.
- 540 Blyth, C.R. (1972). On simpson's paradox and the sure-thing principle. *Journal of the*  
541 *American Statistical Association*, 67, 364–366.
- 542 Carré, D. (1972). Study on development of cnidocysts in gastrozooids of muggiaeae kochi  
543 (will, 1844) (siphonophora, calycophora). *Comptes Rendus Hebdomadaires des Séances de*  
544 *l'Academie des Sciences Serie D*, 275, 1263.
- 545 Carré, D. & Carré, C. (1980). On triggering and control of cnidocyst discharge. *Marine*  
546 *& Freshwater Behaviour & Phy*, 7, 109–117.
- 547 Damian-Serrano, A., Haddock, S.H., & Dunn, C.W. (2020). The evolution of siphonophore  
548 tentilla for specialized prey capture in the open ocean. *PNAS*, 653345.
- 549 Dunn, C.W., Pugh, P.R., & Haddock, S.H. (2005). Marrus claudanielis, a new species of  
550 deep-sea physonect siphonophore (siphonophora, physonectae). *Bulletin of Marine Science*,  
551 76, 699–714.
- 552 Felsenstein, J. (1985). Phylogenies and the comparative method. *The American Naturalist*,  
553 125, 1–15.
- 554 Haddock, S.H., Dunn, C.W., & Pugh, P.R. (2005). A re-examination of siphonophore  
555 terminology and morphology, applied to the description of two new prayine species with  
556 remarkable bio-optical properties. *Journal of the Marine Biological Association of the United*  
557 *Kingdom*, 85, 695–707.
- 558 Harmon, L.J., Weir, J.T., Brock, C.D., Glor, R.E., & Challenger, W. (2007). GEIGER:

- 559 Investigating evolutionary radiations. *Bioinformatics*, 24, 129–131.
- 560 Hessinger, D.A. (1988). Nematocyst venoms and toxins. *The biology of nematocysts* (pp.  
561 333–368). Elsevier.
- 562 Hissmann, K. (2005). In situ observations on benthic siphonophores (physonectae: Rho-  
563 daliidae) and descriptions of three new species from indonesia and south africa. *Systematics  
564 and Biodiversity*, 2, 223–249.
- 565 Ingram, T. & Mahler, D.L. (2013). SURFACE: Detecting convergent evolution from  
566 comparative data by fitting ornstein-uhlenbeck models with stepwise akaike information  
567 criterion. *Methods in ecology and evolution*, 4, 416–425.
- 568 Jombart, T., Devillard, S., & Balloux, F. (2010). Discriminant analysis of principal  
569 components: A new method for the analysis of genetically structured populations. *BMC  
570 genetics*, 11, 94.
- 571 Mackie, G.O., Pugh, P.R., & Purcell, J.E. (1987). Siphonophore Biology. *Advances in  
572 Marine Biology*, 24, 97–262.
- 573 Mapstone, G.M. (2014). Global diversity and review of siphonophorae (cnidaria: Hydro-  
574 zoa). *PLoS One*, 9, e87737.
- 575 Mariscal, R.N. (1974). Nematocysts.
- 576 Mitra, A. (2009). Are closure terms appropriate or necessary descriptors of zooplankton  
577 loss in nutrient–phytoplankton–zooplankton type models? *Ecological Modelling*, 220, 611–620.
- 578 Munro, C., Siebert, S., Zapata, F., Howison, M., Serrano, A.D., Church, S.H., Goetz,  
579 F.E., Pugh, P.R., Haddock, S.H., & Dunn, C.W. (2018). Improved phylogenetic resolution  
580 within siphonophora (cnidaria) with implications for trait evolution. *Molecular Phylogenetics  
581 and Evolution*,
- 582 Pennell, M.W., FitzJohn, R.G., Cornwell, W.K., & Harmon, L.J. (2015). Model adequacy  
583 and the macroevolution of angiosperm functional traits. *The American Naturalist*, 186,  
584 E33–E50.
- 585 Pugh, P. (1983). *Benthic siphonophores: A review of the family rhodaliidai (siphonophora,*

- 586 *physonectae*). Royal Society,
- 587 Pugh, P. (2001). A review of the genus erenna bedot, 1904 (siphonophora, physonectae).
- 588 *BULLETIN-NATURAL HISTORY MUSEUM ZOOLOGY SERIES*, 67, 169–182.
- 589 Pugh, P. & Baxter, E. (2014). A review of the physonect siphonophore genera halistemma
- 590 (family agalmatidae) and stephanomia (family stephanomiidae). *Zootaxa*, 3897, 1–111.
- 591 Pugh, P. & Haddock, S. (2010). Three new species of remosiid siphonophore (siphonophora:
- 592 Physonectae). *Journal of the Marine Biological Association of the United Kingdom*, 90, 1119–
- 593 1143.
- 594 Pugh, P. & Harbison, G. (1986). New observations on a rare physonect siphonophore,
- 595 lychnagalma utricularia (claus, 1879). *Journal of the Marine Biological Association of the*
- 596 *United Kingdom*, 66, 695–710.
- 597 Pugh, P. & Youngbluth, M. (1988). Two new species of prayine siphonophore (caly-
- 598 cophorae, prayidae) collected by the submersibles johnson-sea-link i and ii. *Journal of*
- 599 *Plankton Research*, 10, 637–657.
- 600 Purcell, J. (1981). Dietary composition and diel feeding patterns of epipelagic
- 601 siphonophores. *Marine Biology*, 65, 83–90.
- 602 Purcell, J.E. (1984). The functions of nematocysts in prey capture by epipelagic
- 603 siphonophores (coelenterata, hydrozoa). *The Biological Bulletin*, 166, 310–327.
- 604 Revell, L.J. (2012). Phytools: An r package for phylogenetic comparative biology (and
- 605 other things). *Methods in Ecology and Evolution*, 3, 217–223.
- 606 Revell, L.J. & Chamberlain, S.A. (2014). Rphylip: An r interface for phylip. *Methods in*
- 607 *Ecology and Evolution*, 5, 976–981.
- 608 Siebert, S., Pugh, P.R., Haddock, S.H., & Dunn, C.W. (2013). Re-evaluation of characters
- 609 in apolemiidae (siphonophora), with description of two new species from monterey bay,
- 610 california. *Zootaxa*, 3702, 201–232.
- 611 Skaer, R. (1988). *The formation of cnidocyte patterns in siphonophores*. Academic Press
- 612 New York,

- 613 Skaer, R. (1991). Remodelling during the development of nematocysts in a siphonophore.
- 614 216, 685–689.
- 615 Sugiura, N. (1978). Further analysts of the data by akaike's information criterion and the
- 616 finite corrections: Further analysts of the data by akaike's. *Communications in Statistics-*
- 617 *Theory and Methods*, 7, 13–26.
- 618 Thomason, J. (1988). The allometry of nematocysts. *The biology of nematocysts* (pp.
- 619 575–588). Elsevier.
- 620 Totton, A.K. & Bargmann, H.E. (1965). *A synopsis of the siphonophora*. British Museum
- 621 (Natural History),
- 622 Uyeda, J.C., Zenil-Ferguson, R., & Pennell, M.W. (2018). Rethinking phylogenetic
- 623 comparative methods. *Systematic Biology*, 67, 1091–1109.
- 624 Wagner, G.P. (1996). Homologues, natural kinds and the evolution of modularity. *Ameri-*
- 625 *can Zoologist*, 36, 36–43.
- 626 Werner, B. (1965). Die nesselkapseln der cnidaria, mit besonderer berücksichtigung der
- 627 hydriida. *Helgoländer wissenschaftliche Meeresuntersuchungen*, 12, 1.
- 628 Winemiller, K.O., Fitzgerald, D.B., Bower, L.M., & Pianka, E.R. (2015). Functional
- 629 traits, convergent evolution, and periodic tables of niches. *Ecology letters*, 18, 737–751.